Journal of Power Sources 659 (2025) 238417

Contents lists available at ScienceDirect

Journal of Power Sources

journal homepage: www.elsevier.com/locate/jpowsour

In situ monitoring of impact-induced capacity loss in structural batteries with flexible electronics

Emmanuel A. Ogunniyi [a], Austin R.J. Downey [a,b,*], Subramani Sockalingam [a], Han Liu [c], Simon Laflamme [c]

[a] Department of Mechanical Engineering, University of South Carolina, Columbia, SC, USA
[b] Department of Civil and Environmental Engineering, University of South Carolina, Columbia, SC, USA
[c] Department of Civil, Construction, and Environmental Engineering, Iowa State University, Ames, IA, USA

HIGHLIGHTS

- Capacitive sensors enable real-time impact and battery monitoring.
- Flexible sensors track strain and energy during composite impact.
- Embedded battery and SEC stay functional with minimal impact damage.

ARTICLE INFO

Keywords:
Soft elastomeric capacitor (SEC)
Structural batteries
Impact capacity loss
Battery health monitoring
Multifunctional composite structures
Embedded flexible electronic sensors

ABSTRACT

Integrating soft elastomeric capacitors (SECs) into fiberglass composite laminates presents an innovative approach to monitoring impact energy in structural batteries. In high-performance applications, impact damage can lead to catastrophic battery failures, making real-time sensing crucial for safety and reliability. This study evaluates the performance of SECs in detecting and quantifying impact energy in composites with embedded lithium polymer (LiPo) batteries. Composite laminates with only an embedded SEC as well as composite laminates with SEC adhered to batteries were fabricated and tested to achieve this. Tensile testing, digital image correlation analysis, impact tests, and charge–discharge cycling tests were conducted to examine strain sensing, mechanical behavior, and battery performance of the composite structure. Drop-weight impact tests at 3 J to 18 J revealed a direct correlation between capacitance change and impact severity, with laminates containing embedded batteries exhibiting higher capacitance shifts (up to 4.40 pF) and increased energy absorption (up to 12.30 J) in response to higher deformation. SECs remained functional post-impact. The embedded batteries showed minor electrochemical degradation with increasing impact levels, yet remained operational, confirming their structural resilience. These findings confirm that SECs function as effective real-time impact sensors, enhancing structural health monitoring in aerospace, automotive, and renewable energy applications.

1. Introduction

Embedding batteries in composite structures is a transformative approach that can significantly reduce the overall weight of vehicles and electronic devices [1], enhancing their efficiency and performance [2]. This integration eliminates the need for separate battery compartments, allowing for more compact and streamlined designs [3,4]. These multifunctional materials combine the mechanical properties of composites, such as high strength and stiffness [5], with the electrochemical functions of batteries, enabling them to serve dual roles in various applications paving the way for more sustainable and efficient technologies. This integration improves structural integrity and energy density, particularly in aerospace and automotive applications where weight savings are crucial [1].

Notable challenges of integrating energy storage within structural components include the potential compromise of either mechanical integrity [6] or energy storage efficiency [5] of batteries. Research is mainly focused on enhancing the electrochemical performance of these multifunctional materials while maintaining their structural robustness under various operational conditions. Critical properties such as Tensile properties [7], compression properties [8], bending loads [9], impact damage [10–12], Vibration and Acoustic properties [13] of composites are altered when batteries are embedded towards achieving a

* Correspondence to: A224 300 Main St, Columbia, SC, 29208, USA.
E-mail address: austindowney@sc.edu (A.R.J. Downey).

https://doi.org/10.1016/j.jpowsour.2025.238417
Received 24 February 2025; Received in revised form 19 August 2025; Accepted 15 September 2025
Available online 23 September 2025

multifunctional energy storage composites (MESC). Key issues include optimizing the interface between the structural and electrochemical components to ensure durability and reliability, managing the thermal and mechanical loads to prevent degradation, and developing scalable manufacturing processes [2].

Smart batteries are an advanced type of battery equipped with integrated electronics [14] to manage their operation [15] and enhance their performance [16]. These electronics enable the battery to monitor parameters such as charge level, temperature, and health status, providing real-time data to optimize charging and discharging cycles. Smart batteries can communicate with the host device, ensuring efficient power management and prolonging battery life. Previous studies have demonstrated the use of various sensors in composites, including strain gauges [17], piezoelectric sensors [18], and more. However, these sensors often struggle with conformability and sensitivity when applied to curved battery surfaces, and the structural integrity of the composite laminates is also often compromised [19,20]. Recent advancements in flexible electronics have led to the development of soft elastomeric capacitors (SECs), which offer improved flexibility and performance in health monitoring and measuring impact energy in composites [21]. SECs have emerged as a promising solution due to their flexibility, sensitivity, and ease of integration into composite structures. Consequently, this study aims to investigate the use of SECs to monitor the impact on batteries embedded in fiberglass composites.

The practical implementation of embedding batteries in composite structures, especially for automotive applications where collisions are frequent, necessitates a thorough understanding of impact damage tolerance [22,23]. It is a significant safety concern to determine if embedded batteries alter the energy absorption properties of composites during vehicle collisions [24]. Ensuring that the composite structure provides adequate impact damage tolerance to prevent battery leakage or thermal runaway is also essential [25]. Therefore, monitoring impact energy on embedded batteries in composite materials is critical for ensuring the safety and reliability of high-performance applications where impacts are a concern, such as in aerospace, automotive, and renewable energy sectors. The ability to detect and measure impact energy in real-time can prevent catastrophic failures, such as battery explosions or fires, thereby protecting infrastructure and human lives.

The methodology of this study involved integrating the SECs into fiberglass composite materials, with lithium polymer (LiPo) batteries embedded within these composites. The SECs were adhered to the battery surfaces, enabling real-time monitoring of impact energy. Two samples were utilized: a laminate with only embedded SEC, a control sample, and a laminate with both embedded SEC and battery. The experimental process included fabricating these composite specimens and subjecting them to a tensile test to examine the SEC's strain response embedded in the laminate composite. Controlled impact tests using a drop-weight impact testing machine are then carried out on the samples. Impact energies ranging from 3 J to 18 J were applied, with capacitance changes in the SEC to quantify the impact energy was recorded in real-time. After each impact, the composite's structural integrity is evaluated to determine the extent and shape of internal damage. This assessment clearly visualizes how different impact energies affect the material. The electrochemical performance of embedded batteries is also monitored using charge and discharge cycles before and after each impact, with critical parameters such as voltage and capacity recorded. This process helps assess the influence of impact-induced mechanical stress on the batteries' electrochemical behavior, offering important insights into their long-term reliability and performance under dynamic conditions.

The results demonstrated that the SEC monitored impact energy in both laminate configurations. The capacitance changes observed in the SEC correlated directly with the impact energy level, showing sharp increases in capacitance immediately after impact. This confirmed the SECs' sensitivity and ability to capture real-time data on the structural state of the composites. In laminates with embedded batteries, the results indicated that the batteries influenced the strain distribution within the composite, leading to increased capacitance changes compared to samples without batteries. The charge–discharge tests showed that while the batteries did not experience catastrophic failures, minor performance degradation occurred due to mechanical strain and impact damage, evidenced by a steeper decline in discharge curves. The postmortem examination revealed that as impact energy increased, so did the internal damage, such as delamination around the battery. Overall, the findings confirmed that SECs provide a reliable method for monitoring impact energy on embedded batteries, contributing to developing safer, multifunctional composite materials for high-performance applications.

The contributions of this paper are as follows: (1) This research demonstrates the application of SECs for real-time impact energy monitoring in composite structures with embedded batteries. (2) It enhances safety in high-performance applications by providing a method for early detection of impact-induced damage, helping to prevent catastrophic failures. (3) The study advances multifunctional composite materials by integrating energy storage directly into composite structures while enabling structural health monitoring, expanding the potential applications of flexible electronics in smart materials.

2. Background

This section describes the relevant background needed for this work.

2.1. Energy storage composites

Multifunctional composite structures with embedded batteries represent an innovative approach in material science, merging the roles of energy storage and structural support. By embedding energy storage devices such as batteries within composite materials, these structures can maintain high mechanical performance while simultaneously providing power [26]. This integration is particularly advantageous for applications requiring weight reduction and space efficiency, such as in automotive and aerospace industries [9]. Despite the benefits, embedding batteries can affect the mechanical properties of the host composite, potentially reducing stiffness [7], compression properties [8] and fatigue strength [6,27]. However, advancements in manufacturing techniques and design integration have shown that these impacts can be minimized or even mitigated, with some studies reporting enhancements in properties like vibration damping [13] and bending strength [9]. The success of these multifunctional composites hinges on factors such as the bonding quality between the battery and composite, the type of battery used, and the overall design and manufacturing processes [27,28].

Structural power composites are sophisticated materials engineered to deliver structural integrity and electrical power simultaneously. Integrating energy storage elements, including batteries or capacitor [29], is a common feature in these composites, occurring directly within the composite material [30,31]. The dual functionality is accomplished by modifying the composite matrix or the battery components, enabling them to withstand mechanical loads while simultaneously storing and supplying energy. Carbon fiber and fiberglass are frequently utilized as structural components, which may also serve as electrodes within these composites [32]. A prevalent method includes enhancing the battery in the through-thickness direction or replacing traditional battery materials with composite alternatives [30,33]. This approach can improve mechanical properties while preserving or enhancing electrochemical performance. Structural power composites provide notable advantages regarding weight reduction and spatial efficiency. However, further research is necessary to enhance their performance and durability in operational environments. The challenges encompass the need to ensure consistent mechanical strength and energy capacity and develop scalable manufacturing techniques.

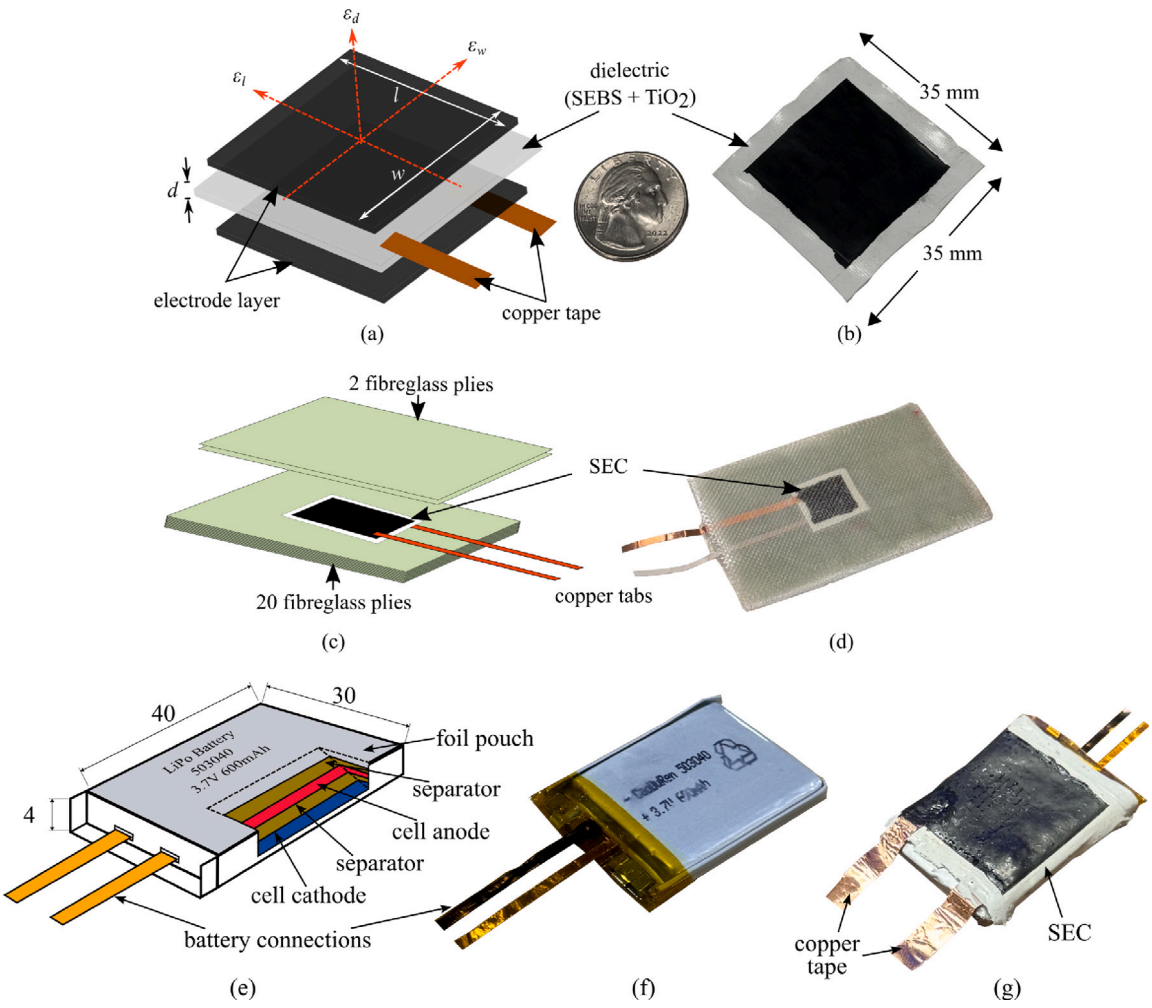

Fig. 1. A soft elastomeric capacitor where (a) is the schematic showing the parallel plate capacitor structure of the SEC with key components and reference axes annotated; and (b) a 35 mm × 35 mm (l × w) SEC; Embedded SEC in laminate composite where (c) shows the schematic of the sample indicating the embedding process, and; (d) is the cured laminate composite with SEC embedded; The battery embedded in composite where (e) is the schematic and dimensions (in mm) of LiPo battery showing components; (f) LiPo battery, and; (g) SEC adhered to the surface of the battery prior to being embedded in the composite.

2.2. Soft Elastomeric Capacitors (SECs)

The SEC has been utilized in various prospective scenarios within structural health monitoring. The sensor has shown effectiveness in monitoring fatigue cracks in steel [34], measuring strain in concretes [35], and quantifying plane strains within hybrid sensor networks [36].

The SEC is an elastomer that can extend up to 500% of its original length in each dimension without yielding, allowing for a linear response in applications that measure at least 25 $\mu\epsilon$. The primary elastomer, styrene–ethylene–butylene–styrene (SEBS), is the fundamental material for constructing the parallel plate capacitor. The dielectric is formulated from the dispersion of titania within the SEBS matrix. Conductive plates are manufactured by dispersing carbon black (CB) particles within a SEBS matrix to create a conductive solution. The conductive solution is applied in layers onto the dielectric, with the accumulation of each layer resulting in a final sheet resistance of about 1 kΩ [37]. The CB+SEBS layer provides considerable environmental durability to the sensor, making it appropriate for prolonged use in diverse conditions [38]. Copper contacts are incorporated to interface with data acquisition systems.

2.2.1. Sensor model

The formulation for the parallel plate capacitor is employed to model the SEC's electrical properties in terms of its physical attributes, as presented in Eq. (1). Here, the capacitance C is related to the ratio of the conductive plates' area, $l \cdot w$, to the distance d between the plates, scaled by the vacuum permittivity ϵ_0 and the dielectric's relative permittivity ϵ_r.

$$C = \epsilon_0 \epsilon_r \frac{l.w}{d} \tag{1}$$

By taking the gradient of the capacitance expression in Eq. (1), the change in capacitance can be derived as shown in Eq. (2), using the reference dimensions annotated in Fig. 1(a). The gradient operator ∇ denotes a sum of partial derivatives in three orthogonal axes of the material, and the Δ operator indicates aggregation over a discrete sensor volume. The formulation is valid when deformation rates within the sensor are consistent.

$$\begin{aligned} \nabla C &= \epsilon_0 \epsilon_r \left(\frac{l}{d} \partial w + \frac{w}{d} \partial l - \frac{lw}{d^2} \partial d \right) \\ &\approx \epsilon_0 \epsilon_r \left(\frac{L}{d} \Delta w + \frac{W}{d} \Delta l - \frac{lw}{d^2} \Delta d \right) \end{aligned} \tag{2}$$

For uniform small strains within the sensor, the derivative can be approximated by a discrete volume shown in Eq. (2). Normalizing this small change by the initial capacitance yields Eq. (3), directly relating strains to changes in sensor capacitance.

$$\frac{\Delta C}{C_0} = \frac{\Delta w}{w} + \frac{\Delta l}{l} - \frac{\Delta d}{d} = \epsilon_w + \epsilon_l - \epsilon_d \tag{3}$$

Using Hooke's stress–strain relationship under the plane stress assumption, substituting ϵ_d in Eq. (3) with the definition in Eq. (4) results in Eq. (5).

$$\epsilon_d = -\frac{\nu}{E}\left(\sigma_l + \sigma_w\right) = -\frac{\nu}{1-\nu}\left(\epsilon_l + \epsilon_w\right) \tag{4}$$

$$\frac{\Delta C}{C_0} = \frac{1}{1-\nu}\left(\epsilon_w + \epsilon_l\right) \tag{5}$$

This provides a physical interpretation of the change in capacitance of the sensor and the material state it adheres to [39].

2.2.2. Impact model

Proof resilience defines a material's ability to absorb strain energy without undergoing permanent deformation. Exceeding this limit leads to the storage of energy as a nonconservative loss. Mechanical energy losses can be monitored to assess the strain energy retained in the plate, as a result of impacts that surpass the plastic deformation threshold. The energy absorbed by the plate can be determined by monitoring the impact velocity of the impactor and the force recorded by the load cell of the impactor [40].

$$E_{\text{sys}}(t) = T_{\text{kinetic}}(t) + U_{\text{gravitational}}(t) - U_{\text{strain}}(t) = 0 \tag{6}$$

During the observation of the impact event from the point of contact until the departure of the impactor from the sample, the simplification presented in Eq. (6) is valid, with minor losses attributed to environmental interactions being disregarded.

$$\Delta U_{\text{strain}} = \Delta T_{\text{kinetic}} + \Delta U_{\text{gravitational}} \tag{7}$$

The total energy stored in the plate (Δ_{strain}) is equivalent to the total change in the mechanical energies of the impactor, as indicated in Eq. (7), during its contact with the composite plate. The load cell signal integration produces the variation in momentum of the impactor. The momentum scaled by the mass of the impactor velocities can be obtained as demonstrated in Eq. (8).

$$\Delta U_{\text{strain}} = m\left(\frac{V_f^2 - V_i^2}{2}\right) + mg\Delta h \tag{8}$$

In this context, V_i and V_f represent the velocities of the impactor before and after the impact event, respectively. Additionally, m denotes the mass of the impactor, g indicates the acceleration due to gravity, and Δh signifies the change in height of the impactor head.

3. Methodology

This section outlines the materials and fabrication processes for producing composite laminates with integrated LiPo batteries. It also details the tensile testing, impact evaluation, and battery charge–discharge procedures conducted to assess their performance.

3.1. SECs in composites

Flexible sensors, such as SECs, are increasingly utilized in diverse areas for real-time health monitoring. These sensors can also be integrated within the composite structure, offering an avenue for continuously assessing its mechanical integrity and detecting issues like strain, stress, or damage.

In this work, initial experimental investigations were designed to test the functionality, sensitivities, and usability of the SECs embedded in fiberglass composite materials. The laminate composite with only embedded SEC was made using 22 plies of woven E-glass material (198 g/m^2) arranged in a [0/90] s fiber pattern. The SEC was positioned on the 20th ply, precisely at the center, and two extra layers of fabrics were placed to cover the sensor as shown in Fig. 1(c). The two top sheet fabrics layers allows the sensor to sense the impact without any hindrance. The resin was infused into the plies using a hand-lay approach, and the vacuum process was used to remove excessive resin in the composite. The final cured sample (Fig. 1(d)) has a dimension of 150 mm by 100 mm with a thickness of 5.5 mm. The embedded SEC is tested under no load first to ensure it is not damaged due to being embedded in the fiber.

3.2. Multifunctional energy storage composite

Fig. 1(e) and (f) illustrate the schematic and the actual image of the LiPo battery sourced from the supplier, which is securely housed in a thin-film protective aluminum pouch. The SEC is adhered to the surface of the battery facing the impactor before being embedded in the composite, as depicted in Fig. 1(g). The battery has a capacity of 600 mAh and operates at a voltage of 3.7 (V), with a voltage range extending from 2.7 to 4.2 (V). The battery connections were replaced with copper tapes measuring 80 mm in length and 4 mm in width. The copper tapes are sufficiently flat to be embedded between the laminates without increasing the overall thickness of the composite. This configuration facilitated the batteries' charging, discharging, and electrical testing prior to their integration into the composites. In addition, it made it possible to do further tests following the embedding of the batteries and any impact events. The connection points were secured using hot melt glue to mitigate the risk of short circuits.

The laminate was fabricated using 22 layers of plain weave E-glass woven roving (198 g/m^2), oriented in a [0/90] s pattern. A cut-out, measuring 40 mm × 30 mm, was made in the central 18 layers to accommodate a LiPo battery and SEC, with the cut-out size matching the dimensions of the battery. After placing the battery within the laminate, two additional layers of fabric, without cut-outs, were added on the top and bottom surfaces to encapsulate the battery fully, as described in Fig. 2(a). The preform was infused with epoxy resin at room temperature using the vacuum bag resin infusion (VBRI) technique, applied under a pressure of −0.95 bar, as shown in Fig. 2(b), with the complete schematic of the process depicted in Fig. 2(c). The resin system consisted of a Totalboat Model 510 825 high performance epoxy resin (part 1) mixed with a high performance fast hardener (part 2) in a 2:1 weight ratio. After resin infusion, the laminate was cured at 24 °C for 24 h. The final laminate thickness was 5.5 mm, and the fiberglass content was 55% by volume. Table 1 provides the battery and laminate composite structure's nominal mass density and energy density. Although the overall energy density of the composite structure was lower than the bare battery, the multifunctional design offered additional benefits such as structural integrity.

3.3. Tensile tests

In-plane tensile tests were conducted on composite laminate with embedded SEC and composite laminate with embedded battery and SEC (Fig. 3(a)) before impact testing, following the guidelines of ASTM D3039. The cyclic loading procedure was designed to evaluate the performance of the SEC as a strain-sensing material embedded in composite material, as shown in Fig. 3(c). The cyclic load was a 0.15 Hz harmonic excitation in tension mode between 3 kN and 6 kN for three cycles using a dynamic testing machine (MTS with Model No. 609.25A-01), having a maximum loading capacity of 250 kN.

To capture the surface strain field over the centrally positioned SEC and the battery of the specimen under cyclic tensile loading, digital Image Correlation (DIC) was employed. The purpose of the DIC measurements was to compare the surface strain experienced at the embedded location with the measurements of the SEC and strain from the dynamic testing system. A 5 MP camera, operated through VIC-snap software (Correlated Solutions), was used to capture the images, and the data were processed with VIC-2D software using a subset size of 35 and step size of 7, which provided a good balance between spatial resolution and noise reduction for the speckle pattern employed. Strain data from the SEC, the dynamic testing system, and the DIC were collected simultaneously during the tests. For the DIC data analysis, only the vertical strain component, ϵ_y, was considered in processing the results.

Table 1
Physical and electrical properties of the laminate composite without and with the LiPo battery. Properties of battery also given.

Samples (with SEC)	Average weight (g)	Average mass density (kg/m^3)	Energy density (Wh/kg)	Energy density (Wh/L)
Laminate without battery	140	1690	–	–
Laminate with battery	135	1630	15.7	26.9
LiPo battery	10.0	2080	220	440

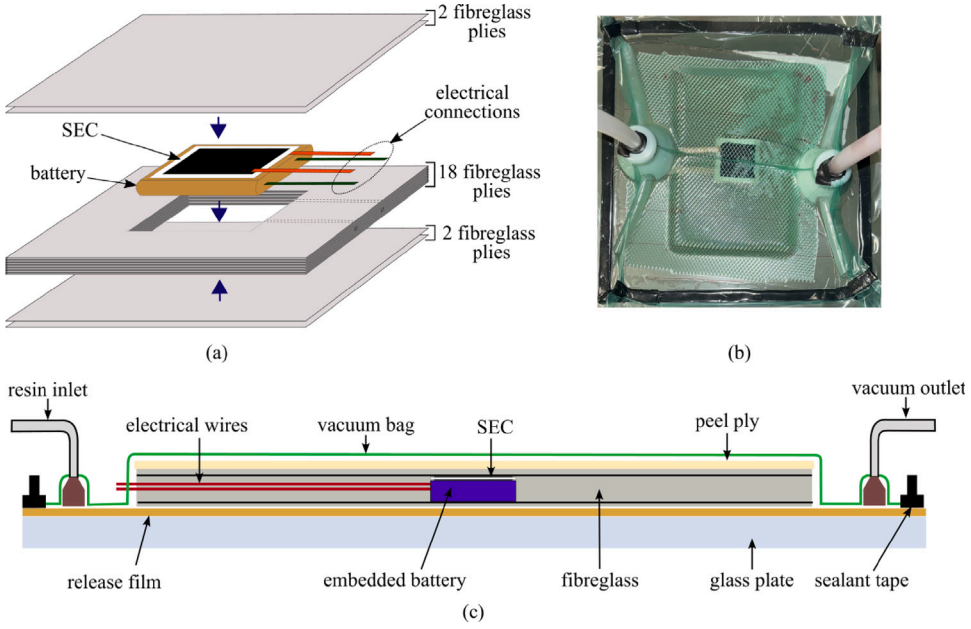

Fig. 2. Multifunctional energy storage composite fabrication technique where (a) shows the schematic of the laminates, battery and SEC indicating the embedding direction, and; (b) and (c) are the actual and schematic of the vacuum bag resin infusion (VBRI) technique used to preform the sample.

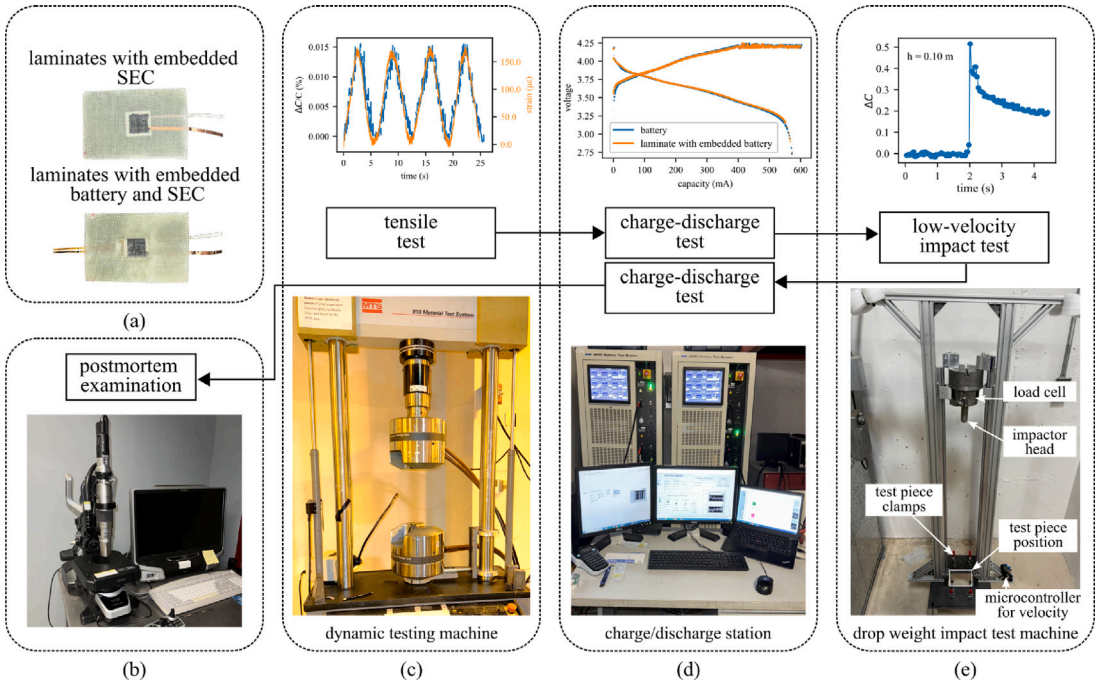

Fig. 3. Experimental setup illustrating (a) the two laminate composite configurations with an embedded battery and SEC; (b) a digital microscope for assessing damage extent; (c) dynamic testing system for tensile test on samples; (d) a charge–discharge test station, and; (e) a drop-weight impact testing system.

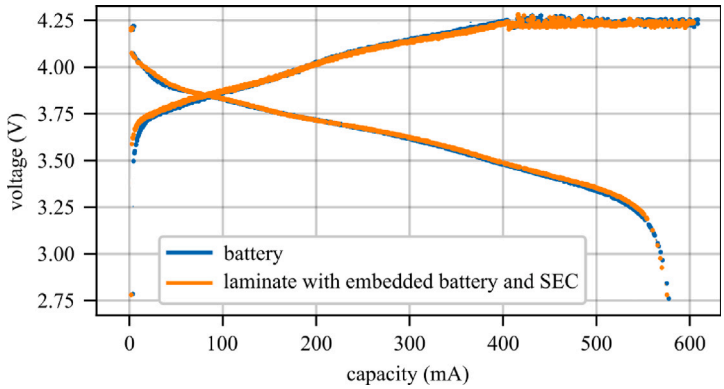

Fig. 4. Initial charge and discharge test on bare and embedded lithium polymer (LiPo) batteries in laminates samples.

3.4. Charge and discharge tests

Charge–discharge cycling tests were conducted before and after subjecting the cells to impact loading to evaluate the impact of mechanical damage on the electrochemical performance of embedded pouch cells. These tests aimed to assess any degradation in capacity or performance resulting from mechanical impacts that did not result in catastrophic failures, such as internal short circuits or significant heat generation. Fig. 3(d) provides a detailed overview of the testing system.

The charge–discharge cycling procedure was performed using a NHR 9200 battery test system. The embedded batteries were cycled in the laminate composite structures following a constant-current, constant-voltage (CCCV) scheme at 1C (600 mAh), with voltage limits between 4.2 V and 2.75 V and a C/25 cutoff. Key parameters such as voltage, current, and cell capacity were recorded during the cycling process to monitor performance changes. Testing conducted on bare and embedded lithium polymer (LiPo) batteries, following the ISO 12405-4 standards, is depicted in Fig. 4. The capacity–voltage profiles for both the embedded and bare cells were nearly identical, suggesting that the embedding process had minimal influence on battery performance.

3.5. Impact tests

The experimental testing aimed at evaluating impact energy in laminate samples was carried out by the ASTM D7136/D7136M standard, which outlines procedures for determining the impact resistance of composite materials. The setup, illustrated in Fig. 3(e), enabled data collection regarding the impact energy absorbed by the laminate panels during impact, which was compared to the changes observed in SEC's capacitance. It was anticipated that when the material's proof resilience was exceeded, a significant change in capacitance would occur, signaling that the sensor had detected a change in the material configuration. The drop tower is designed to adhere to ASTM guidelines; an exception was made for the impactor mass, which was set at 7.5 kg, outside the standard range. The impactor head met the requirement for a hemispherical shape, and the support fixture dimensions followed the prescribed guidelines as described in [40]. The load cell, a Honeywell pancake-type model 43, was sampled at 15 kHz, which aligns with the ASTM standard. The specimens, each measuring 150 mm in length and 100 mm in width, were mounted on a rigid base of dimensions 137.5 mm × 87.5 mm, with all edges fully clamped to ensure no movement during testing. The battery positioned centrally on each specimen is marked as the designated impact location. Each specimen underwent a single impact, and successive impacts were prevented.

Capacitance values for the SEC were recorded using a B&K Precision model 891 at a test frequency of 1 kHz, with a sampling rate of 45 S/s and an error margin of 2% for the SEC's capacitance range (100 pF). Due to the dynamic nature of the impact tests, special care was taken to prevent mechanical disturbances from affecting the capacitance measurements. Tri-axial cables (Video Triax, RG11, 15 Stranded, CL2X) were used to minimize signal interference. The ground plane of the SEC was attached to the sample, a practice extended to all equipment in contact with the sample, including the impactor, drop tower, and other equipment, ensuring optimal signal isolation.

For safety reasons, all embedded batteries were charged to about 60% state of charge (SOC) before impact tests. Impact tests on the laminates with only embedded SEC were performed at energy levels of 7.4, 8.8, 11.0, 14.7 and 18.4 J, while for the laminates with both embedded battery and SEC, impact test was conducted at levels of 3.7, 7.4, 8.8, 11.0 and 14.7 J, with each energy level repeated twice to ensure the reproducibility of results. While this may limit the statistical power of the results, the approach of using two repetitions is consistent with pilot or proof-of-concept studies, and it is consistent with similar preliminary studies in composite impact research involving destructive mechanical testing of embedded energy systems, where initial demonstration of feasibility and trends is prioritized [11,12] before scaling up to larger experimental campaigns. The upper limit for impact energy on a laminate with an embedded battery was set at 14.7 J to prevent battery exposure on the specimen surface.

A microscope was utilized to assess the laminate specimens before and after impact testing. Impact damage was quantified using the projected surface damage area between the fiberglass layers and the LiPo battery, as well as the indentation depth. The projected surface damage was measured around the impact location. Indentation depth was determined by measuring from the top of the undamaged face sheet to the most severely damaged point on the impacted face sheet.

4. Results

This section presents the results of tensile tests, impact tests, and charge–discharge cycling, along with a post-mortem analysis of the tested samples. It also explores the effectiveness of SECs in monitoring impact energy and their implications for assessing the condition of embedded batteries within composite structures.

4.1. Tensile tests on composite samples

The in-plane tensile tests on composite laminates embedded with the SEC and the configuration incorporating both the SEC and a LiPo battery revealed distinct differences in capacitance change and strain response. In the laminate with only an embedded SEC shown in Fig. 5(a), the capacitance change ($\Delta C/C$) followed a cyclic pattern corresponding to the harmonic loading. The SEC measured a capacitance change of up to approximately 0.015%, with a corresponding peak strain of around 180 $\mu\epsilon$ recorded by the dynamic testing system. The strong correlation between capacitance change and strain demonstrates that the SEC performed effectively as a strain sensor in an embedded

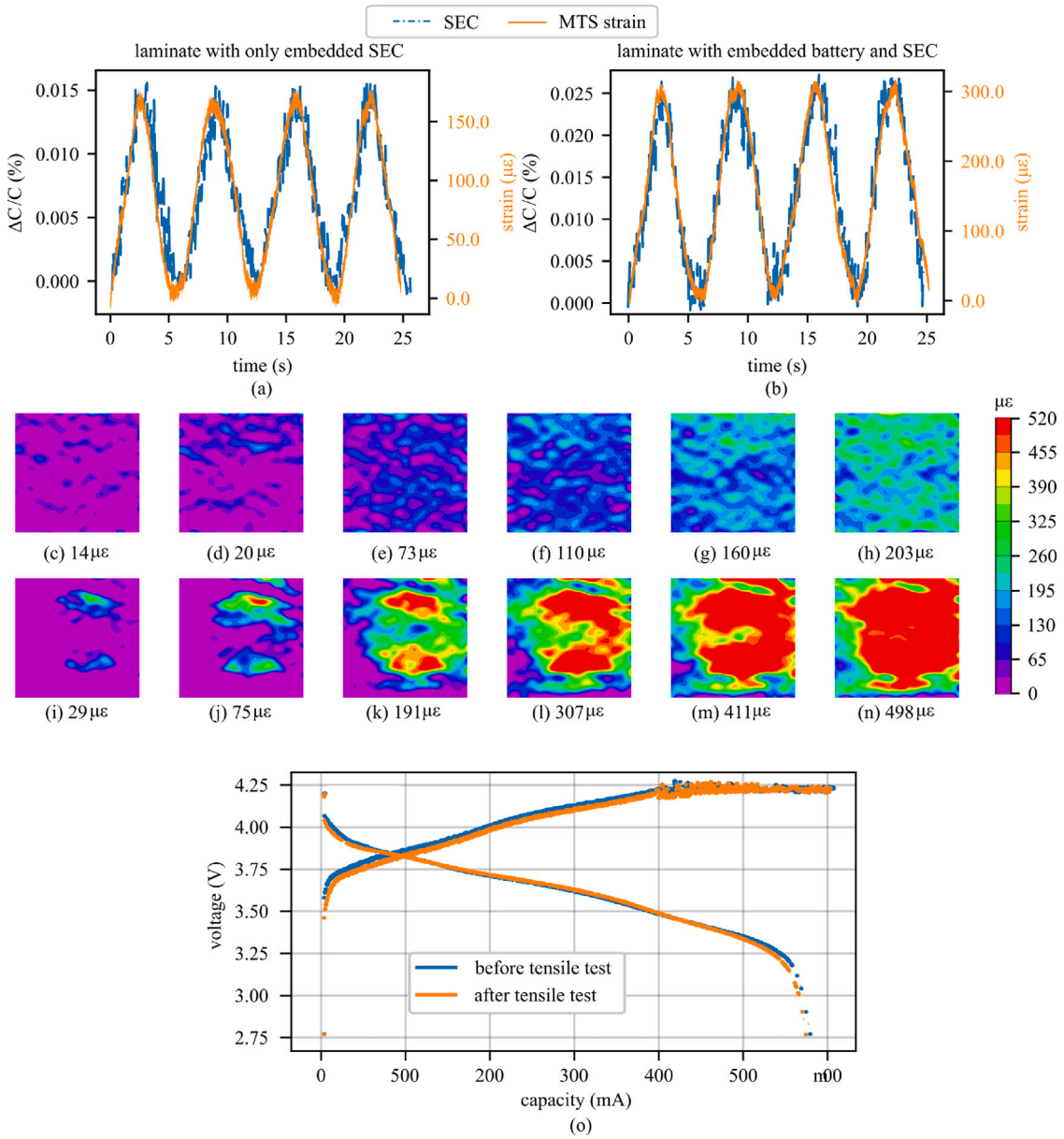

Fig. 5. Tensile test results illustrating capacitance change and strain measurements for: (a) a laminate with an embedded SEC; (b) a laminate with embedded battery and SEC; (c)–(h) strain field at the center point of the laminate with only an embedded SEC; (i)–(n) strain field at the center point of the laminate containing both an embedded battery and SEC, and; (o) Charge and discharge test on laminate sample with embedded battery after tensile test.

state. The uniform strain distribution indicated a smooth response to the applied cyclic loading.

The laminate with both embedded battery and SEC in Fig. 5(b) exhibited a similar cyclic pattern. However, the capacitance change increased to approximately 0.025%, and the peak strain reached around 320 $\mu\epsilon$, almost double that of the configuration without the battery. This increase is primarily attributed to the mechanical stiffness introduced by the battery, which altered the internal load distribution, leading to localized areas of higher strain detected by both the SEC and the dynamic testing system. Additionally, the battery may have caused some interference with the SEC, contributing to the larger capacitance variation, as the SEC is sensitive to both strain and electrical interference from nearby components, the reason for the initial grounding of the entire setup.

DIC results provided further insight into the strain behavior in both configurations at the exact center position with the battery and SEC. For the laminate with only the SEC shown in Fig. 5(c) to (h), DIC showed a gradual, uniform increase in strain. At the lowest average strain level of 14 $\mu\epsilon$ (Fig. 5(c)), the strain was evenly distributed across the specimen. As loading increased, reaching an average of 203 $\mu\epsilon$ at the highest load (Fig. 5(h)). The gradual uniform distribution confirms the SEC's ability to sense strain without introducing significant mechanical interference.

However, in the laminate composite with both the SEC and battery in Fig. 5(i) to (n), the strain distribution was much less uniform. At lower strain levels, Fig. 5(i) with 29 $\mu\epsilon$, strain concentration occurred near the battery but was less evenly distributed than the configuration without the battery. As strain increased, DIC analysis revealed significant strain localization around the battery. By Fig. 5(n) at 498 $\mu\epsilon$, the strain was heavily concentrated near the battery, with values far exceeding those observed in the laminate without the battery. This indicates that the battery's stiffness restricted the free distribution of strain across the laminate, leading to increased mechanical stress in surrounding areas. The concentrated strain in the area with the battery monitored with DIC is also greater than the overall tensile strain

measured by the dynamic testing system on the sample, which confirms the localization of stress around the battery.

4.2. Charge/discharge after tensile tests

The charge–discharge tests on the laminate composite sample with an embedded battery, shown in Fig. 5(o), reveal changes in the battery's electrochemical performance after undergoing tensile testing. Before the tensile test, the charge–discharge curve exhibits behavior typical of a battery, with the charge voltage reaching 4.2 V and the discharge voltage decreasing steadily to 2.7 V over a capacity of approximately 600 mAh. This consistent trend reflects normal battery operation under the constant-current, constant-voltage (CCCV) charging scheme, with no evident issues in capacity or voltage.

Following the tensile test, the battery's performance changed only a little. The discharge curve declines sharply towards the end and the overall capacity drops. Although the battery still reaches the 4.2 V charge limit, the steeper decline in the discharge curve towards the end suggests an increased internal resistance or possible structural damage. This indicates that the mechanical strain from the tensile loading affected the battery's internal components, leading to probable performance degradation. The reduced capacity, visible in the smaller area under the post-tensile curve, demonstrates the battery's diminished ability to hold and deliver charge. While the battery did not experience catastrophic failures, such as an internal short circuit or excessive heat generation, the tensile load caused a slight decrease in electrochemical efficiency. This is evident in the altered voltage profile, where the battery no longer maintains the same energy output as before the mechanical strain.

4.3. Impact energy correlation with SEC capacitance change

4.3.1. Laminates with only embedded SEC

The impact tests on laminate composites embedded with SEC revealed how the sensor responds to varying energy levels. Fig. 6(a) to (e) illustrate the capacitance changes (ΔC) of the SEC at five different impact heights: 0.10 m, 0.12 m, 0.15 m, 0.20 m, and 0.25 m, each corresponding to increasing impact energy applied by a 7.5 kg impactor. In all cases, a sharp spike in capacitance occurred shortly after impact, followed by stabilization. As the impact height increased, the magnitude of the spike also increased, indicating the sensor's ability to detect higher energy levels. At the first impact height of 0.10 m (Fig. 6(a)), the capacitance change reached approximately 0.5 pF at the 2-s mark, signaling the point of impact. A similar trend is seen at higher impact levels, with capacitance change correlating to impact level.

The force profiles recorded by the load cell, presented in Fig. 6(k) to (o), also demonstrate a consistent increase in peak force with impact height. At the initial height of 0.10 m, the force peaked at approximately 300 N, while at 0.25 m, it reached nearly 450 N. These force curves were symmetric and steep, reflecting the rapid application and release of force during impact. The alignment between the force profiles and the capacitance changes confirms the SEC's ability to detect real-time impacts across different energy levels. Non-destructive inspection (NDI) after the impact event of the samples shown in Fig. 6(f) to (j) visually represents the delamination damage corresponding to each impact height. As the impact energy increased, so did the damage, with the 0.25 m impact (Fig. 6(j)) showing a delamination area extending up to 10 mm^2 from the impact center. This progression mirrors the capacitance increases, confirming the SEC's ability to sense structural changes tied to impact severity.

4.3.2. Laminates with embedded SEC and battery

The impact tests on the laminate composite with an embedded SEC and battery show a few differences from those without a battery. These tests were conducted from impact heights of 0.05 m, 0.10 m, 0.12 m, 0.15 m, and 0.20 m, with no test performed at 0.25 m due to concerns about battery safety at higher impact levels. Fig. 7(a) to (e) reveal a consistent increase in capacitance change (ΔC) as the impact height increases. At 0.05 m (Fig. 7(a)), the capacitance change peaks around 1.25 pF, while at 0.20 m (Fig. 7(e)), it reaches approximately 4.5 pF. This higher response in capacitance change compared to the laminate without a battery suggests that the embedded battery alters strain distribution, concentrating strain on the SEC during impact due to the increased structural stiffness.

The force data in Fig. 7(k) to (o) further highlight differences. Peak forces are significantly lower in the laminates with an embedded battery. At an impact height of 0.10 m, the peak force is around 225 N, while the laminate without the battery registered 300 N at the same height. This reduction indicates that the battery absorbs some of the impact energy, reducing the force experienced by the laminate. However, the presence of the battery also results in an indentation in the sample after impact. At 0.20 m (Fig. 7(o)), the indentation depth reaches about −2.1 mm, which was not experienced in the laminate without the battery. NDI of the samples in Fig. 7(f) to (j) shows an increasing delamination area with impact height, as observed in the laminate without a battery. However, delamination is generally larger in the configuration with the battery, suggesting that the battery influences damage propagation by affecting energy dissipation. Table 2 summarizes the data described in Figs. 6 and 7.

Fig. 8(a) and (b) detailing the comparison of the capacitance change and peak force between the two laminates configurations shows that the laminate with the embedded battery consistently exhibits higher capacitance changes across all impact heights reflecting localized strain amplification around the battery, while the peak forces are lower, indicating the battery's effect on energy absorption, redistributing the impact force and altering the strain response of the laminate during impact.

4.4. Impact energy and energy absorption

The performance of laminates embedded with SECs, both with and without batteries, can be assessed under controlled impact conditions by analyzing impact energy and energy absorption metrics. This evaluation involves calculating impact energy, determining energy absorption, and examining their relationship with key parameters such as force, deflection, and capacitance variations. The impact energy was determined using the potential energy equation, $E = mgh$, where m is the impactor mass (7.5 kg), g is the acceleration due to gravity (9.81 m/s^2), and h is the drop height. As shown in Table 3, impact energy increased linearly with height, reaching a maximum of 18.39 J at 0.25 m. This trend remained consistent across both laminate configurations, as impact energy is solely dependent on the mass of the impactor and the height from which it is dropped.

ΔC is observed to increase with impact energy for both laminate configurations as depicted in Fig. 8(c). The laminate with the embedded battery and SEC exhibits a more pronounced increase in ΔC compared to the laminate with only the SEC. This suggests that the battery's presence influences the composite's strain response, likely due to localized stiffness variations and stress concentrations around the embedded battery. The SEC in both configurations successfully detects the deformation caused by impact, but the higher ΔC values in the battery-embedded configuration indicate a more significant deformation in the sample.

Energy absorption values were calculated for laminates with embedded SEC and those with embedded SEC and battery. For laminates with only SEC, energy absorption ranged from 3.80 J at a height of 0.10 m to 11.24 J at 0.25 m. In the case of laminates with embedded SEC

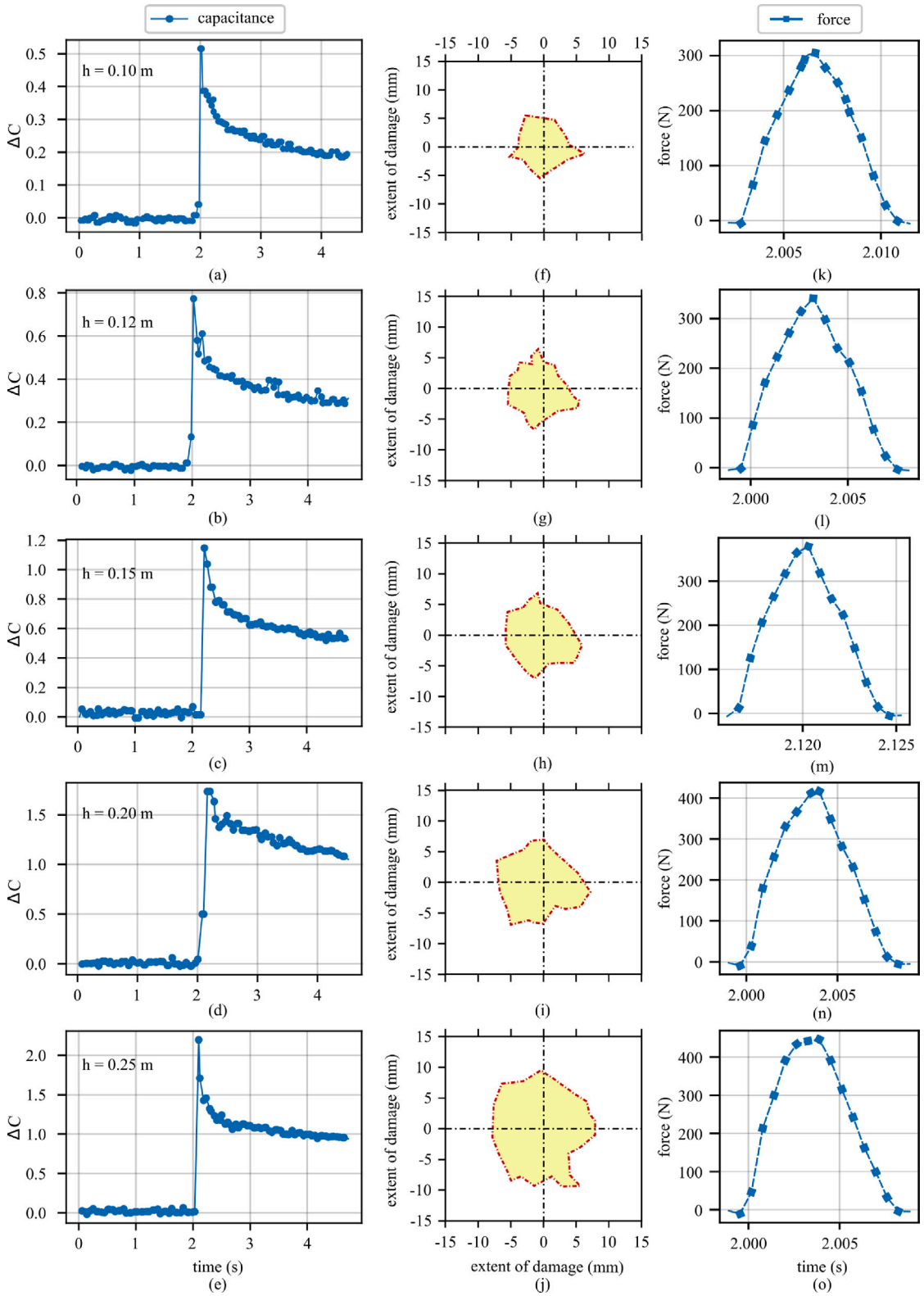

Fig. 6. Impact test on laminate composite with embedded SEC where (a)–(e) shows SEC capacitance change in response to impact; (f)–(j) depicts the extent of damage caused by impact on the laminate, and; (k)–(o) force response from the impact.

and battery, energy absorption values were slightly higher at equivalent heights due to the additional stiffness introduced by the battery, which influenced strain distribution and energy dissipation (Fig. 8(d)), which was noticeable in the damage induced in the laminate. The computed values are summarized in Table 3.

4.5. Charge/Discharge after impact

Fig. 8(e) presents the charge–discharge curves for the laminate composite with an embedded battery at various stages, including before and after tensile tests, as well as following impact tests at different

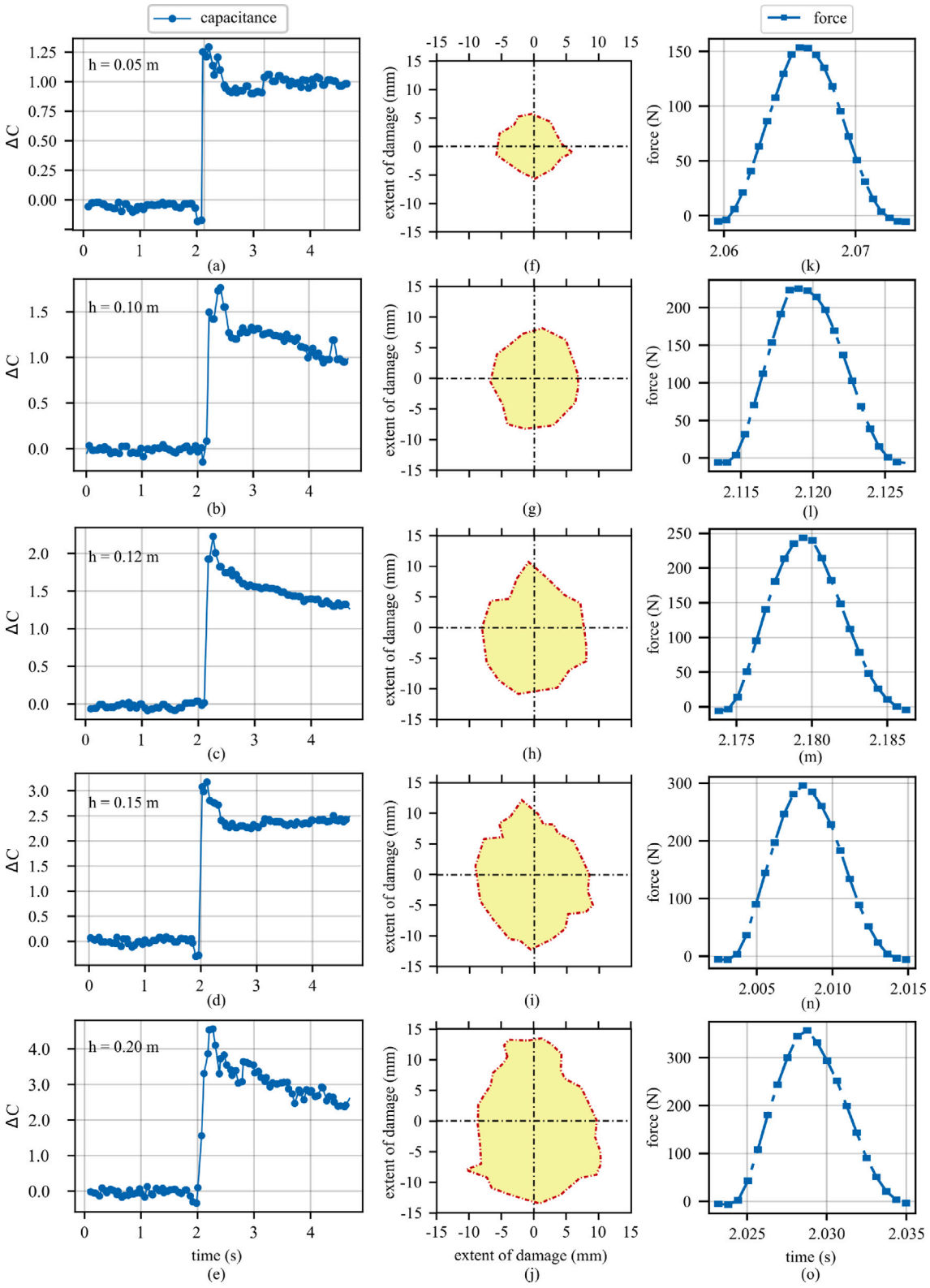

Fig. 7. Impact test on laminate composite with embedded SEC and battery where (a)–(e) shows SEC capacitance change in response to impact; (f)–(j) depicts the extent of damage caused by impact on the laminate, and; (k)–(o) force response from the impact.

heights of 0.05 m, 0.10 m, 0.12 m, 0.15 m, 0.20 m. These profiles reveal critical insights into how mechanical stress and impact energy affect the battery's electrochemical performance.

Before the tensile test, the battery demonstrates a smooth charging process, reaching a maximum voltage of 4.2 V and a stable discharge curve, dropping to approximately 2.75 V over a capacity close to 600 mAh. This behavior reflects the battery's normal performance, providing a baseline for comparison. After the tensile test, the battery shows a small deviation in performance, particularly during the discharge phase. The discharge curve drops more rapidly at higher capacities than

Table 2
Summary of data obtained from impact test on laminate with only SEC and laminate with battery and SEC.

Impact height (m)	ΔC (pF)		Peak force (N)		Indentation depth (mm)
	Sec	Battery and Sec	Sec	Battery and Sec	(battery and Sec)
0.05	–	1.25	–	150	0.5
0.10	0.52	1.70	300	225	0.8
0.12	0.77	2.20	330	245	1.2
0.15	1.17	3.10	380	300	1.6
0.20	1.70	4.40	405	345	2.1
0.25	2.20	–	430	–	–

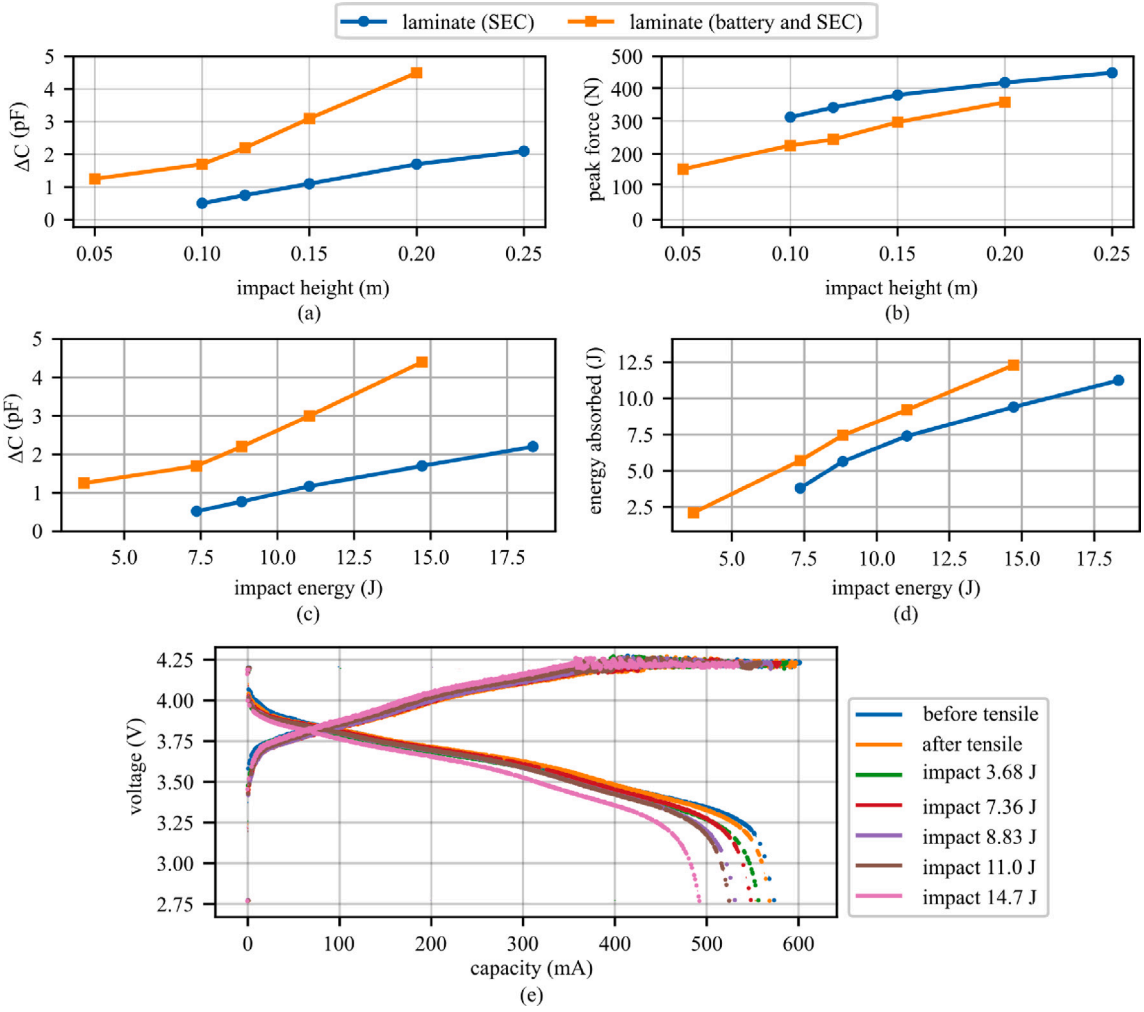

Fig. 8. Comparison of the laminate with only SEC and laminate with embedded battery and SEC in terms of (a) capacitance change; (b) peak force at different impact heights; Comparison of the laminate with only SEC and laminate with embedded battery and SEC in terms of (c) capacitance change; (d) energy absorbed at different impact energy, and; (e) Charge and discharge test on laminate sample with embedded battery before tensile, after tensile, and at impact height 0.05 m, 0.10 m, 0.12 m, 0.15 m and 0.20 m.

Table 3
Impact energy, capacitance change, and energy absorption of laminates with embedded SEC and battery.

Impact height (m)	Impact energy (J)	Laminate (SEC)		Laminate (battery and SEC)	
		ΔC (pF)	Energy absorbed	ΔC (pF)	Energy absorbed
0.05	3.68	–	–	1.25	2.10
0.10	7.36	0.52	3.80	1.70	5.70
0.12	8.83	0.77	6.12	2.20	7.45
0.15	11.04	1.17	7.80	3.00	9.20
0.20	14.72	1.70	9.40	4.40	12.30
0.25	18.34	2.20	11.24	–	–

the pre-tensile condition, indicating an increased internal resistance or minor internal damage. This suggests that although the battery remains functional, the tensile stress has impacted its electrochemical behavior, likely through slight structural deformation or increased contact resistance, which limits its ability to sustain voltage during discharge.

In the event of impacts, the battery's performance progressively deteriorates. Following impact from 0.05 m, the discharge curve shows a small but noticeable reduction in the battery's ability to maintain voltage at higher capacities, indicating the onset of damage. This trend becomes more pronounced with impacts at 0.10 m and 0.12 m, where the discharge curve experiences more significant voltage drops at lower capacities. These changes suggest that impacts at these heights introduce further internal damage, likely in the form of minor delamination or degradation of internal components, which hinders the battery's ability to store and release energy efficiently. For impacts at 0.15 m and 0.20 m, the degradation in battery performance becomes substantial. The discharge curves for these impact heights show a rapid voltage drop even at moderate capacities, indicating a marked increase in internal resistance and possible structural damage. The observed voltage drops and capacity loss after impact are consistent with internal mechanical damage such as electrode fracture [11], delamination [41], structural disruption [42], or electrolyte dislocation [43]. However, these deductions are based on indirect electrochemical evidence. Direct validation using advanced techniques such as electrochemical impedance spectroscopy (EIS) and X-ray computed tomography (X-CT) is recommended for future studies to confirm the specific nature and extent of internal damage. The fact that the battery can still function post-impact, though with reduced capacity, suggests that the internal damage is not catastrophic but is sufficient to limit its efficiency and longevity. Aside from battery capacity loss, impacts can induce localized temperature rises, the brief duration (milliseconds) and low to moderate levels (3.7 J to 18.4 J) used in this study are not expected to produce significant thermal effects on either the embedded batteries or the SECs. This is supported by literature indicating that battery performance and elastomeric sensor properties remain stable, and are known to tolerate minor, transient mechanical stress without significant thermal sensitivity at the tested energy levels [44,45].

Throughout the stages, the charge curves remain relatively consistent, reaching 4.2 V, indicating that the battery can still charge to its full voltage. However, the degradation observed in the discharge profiles highlights how mechanical impacts and tensile stresses progressively reduce the battery's energy-delivery capability. The increasing difficulty in maintaining voltage during discharge, particularly after higher impact energies, indicates the accumulation of internal damage that directly affects the battery's capacity and efficiency. The results demonstrate that while the battery can tolerate minor mechanical deformations, such as tensile stress, repeated or severe impacts, especially at impact energy above 8 J may lead to considerable performance degradation.

The experiment shows that impact affects battery capacity by causing internal mechanical and structural damage. This includes damage to the active material or electrode layers, reducing the surface area available for energy storage. Impacts can also cause damage to the separator, which can lead to short circuits and explosions [46,47], for this reason, batteries were not tested to failure. Furthermore, severe impacts generate heat that may result in electrolyte leakage, further limiting the efficiency of ion exchange through the separator, and resulting in a reduction in capacity [48]. Additionally, mechanical stress can weaken the contact between battery layers, and localized heating from impacts can cause thermal degradation of sensitive materials.

4.6. SEC post-impact functionality

The performance of SECs after impact is crucial for assessing their reliability in structural health monitoring and impact energy evaluation. Experimental results demonstrate that embedded SECs remain functional despite significant impacts, with their capacitance following a characteristic recovery trend. While an initial spike occurs immediately after impact, the sensors stabilize shortly thereafter, highlighting their resilience to mechanical stress. However, embedded SECs may exhibit non-linear capacitance variations at higher impact energy levels, indicating that internal strain distribution may change their baseline capacitance while still embedded in the composite. The non-linear variations and baseline capacitance shifts in SEC capacitance are attributed to non-uniform strain distributions, as supported by theoretical models and validations in prior experimental studies using DIC and finite element analysis. Such baseline shifts have been reported as a result of evolving strain fields and structural damage. These findings confirm that localized damage or stress concentrations from the battery or composite can induce non-linear sensor responses [49,50]. Post-impact microscopy suggests that delamination and localized strain concentrations contribute to these variations.

Post-impact assessment reveals that capacitance changes in SECs embedded alongside batteries are higher than in battery-free laminates. This is attributed to localized strain amplification, as the rigid battery structure acts as a stress concentrator during impact. Repeated impact testing confirms that SECs retain monitoring capabilities over multiple impact events, though baseline capacitance values gradually shift. In this work, the shift is likely due to accumulated mechanical wear or minor damage to the battery and composite material in the area of impact [21]. Despite these changes, SECs remain effective as embedded sensors within composite structures. Furthermore, post-impact analysis highlights their role as indicators of energy dissipation, as capacitance readings strongly correlate with observed delamination and indentation damage. This provides valuable insights into the composite's ability to absorb and distribute impact energy without catastrophic failure. Given the absence of abnormal battery behavior and the stable sensor response post-impact, as well as established findings that moderate, short-term temperature fluctuations do not substantially affect the materials studied, the integration of temperature sensors to monitor the SEC and battery was deemed unnecessary for the present work.

5. Conclusion

This study investigates using soft elastomeric capacitors (SECs) for real-time impact energy monitoring in fiberglass composite laminates with embedded lithium polymer (LiPo) batteries. The research evaluates the SECs' ability to detect impact-induced strain, quantify impact energy, and assess structural integrity.

Embedded batteries alter strain distribution, requiring sensing solutions that conform to complex composite structures. SECs, due to their flexibility and high sensitivity, can effectively monitor impact-induced deformations, overcoming the limitations of conventional sensors. Two types of laminates were fabricated to evaluate the SEC performance: one with only SEC and another with embedded SEC and an embedded battery. Tensile tests under cyclic loading (0.15 Hz, 3–6 kN) were used to assess SEC response to mechanical strain, while DIC analysis captured strain distribution patterns. Drop-weight impact tests (3–18 J) examined capacitance variations in response to impact severity, and post-impact charge–discharge tests evaluated battery degradation.

The study demonstrates that SECs reliably correlate capacitance changes with impact severity and maintain functionality post-impact, confirming their effectiveness as embedded sensors. Higher capacitance changes (up to 4.40 pF) were observed in laminates with embedded batteries, indicating localized strain amplification. Additionally, energy absorbed in battery-embedded laminates reached 12.30 J, surpassing that of SEC-only laminates. DIC results validated SEC readings, showing concentrated strain near embedded batteries. Despite minor sensitivity shifts at higher impact levels, SECs remained functional. Charge–discharge tests revealed slight battery performance degradation but no catastrophic failures. Although temperature monitoring was not incorporated in this work because the tests were carried out under low

to moderate energy levels, future investigations may integrate thermal sensors to evaluate any subtle coupled effects of heat on sensor and battery behavior under extreme or repeated impact loading.

These results highlight SECs' potential for SHM in aerospace, automotive, and energy applications, where real-time impact detection is crucial. However, non-linear signal shifts suggest that long-term measurement accuracy should be further evaluated under repeated impact loading to enhance the statistical robustness of impact response data. Future work should employ advanced characterization methods, such as EIS and X-CT, to directly characterize internal damage mechanisms following impact events. This research advances multifunctional smart materials by demonstrating SECs as dual-purpose sensors for impact detection and strain monitoring. Future studies should optimize sensor placement and explore scalable manufacturing processes for industrial adoption. Additionally, long-term durability assessments and investigations into alternative battery chemistries will enhance the integration of SECs into next-generation structural energy storage systems.

CRediT authorship contribution statement

Emmanuel A. Ogunniyi: Writing – original draft, Methodology, Investigation, Conceptualization. **Austin R.J. Downey:** Writing – review & editing, Supervision, Methodology, Funding acquisition. **Subramani Sockalingam:** Writing – review & editing, Methodology. **Han Liu:** Writing – review & editing, Resources. **Simon Laflamme:** Writing – review & editing, Resources.

Declaration of competing interest

The authors declare the following financial interests/personal relationships which may be considered as potential competing interests: Austin Downey reports financial support was provided by National Science Foundation. If there are other authors, they declare that they have no known competing financial interests or personal relationships that could have appeared to influence the work reported in this paper.

Acknowledgments

The National Science Foundation, United States provided support for this work through Grant CPS-2237696. The National Science Foundation's support is sincerely thanked. The authors' opinions, results, conclusions, and recommendations in this material are their own and do not necessarily reflect the views of the National Science Foundation.

Data availability

The data used in this study has been incorporated into the manuscript.

References

[1] Till Julian Adam, Guangyue Liao, Jan Petersen, Sebastian Geier, Benedikt Finke, Peter Wierach, Arno Kwade, Martin Wiedemann, Multifunctional composites for future energy storage in aerospace structures, Energies 11 (2) (2018) 335, http://dx.doi.org/10.3390/en11020335.

[2] Purim Ladpli, Raphael Nardari, Fotis Kopsaftopoulos, Fu-Kuo Chang, Multifunctional energy storage composite structures with embedded lithium-ion batteries, J. Power Sources 414 (2019) 517–529, http://dx.doi.org/10.1016/j.jpowsour.2018.12.051.

[3] Tianwei Jin, Gerald Singer, Keyue Liang, Yuan Yang, Structural batteries: Advances, challenges and perspectives, Mater. Today 62 (2023) 151–167, http://dx.doi.org/10.1016/j.mattod.2022.12.001.

[4] Leif E Asp, Mats Johansson, Göran Lindbergh, Johanna Xu, Dan Zenkert, Structural battery composites: a review, Funct. Compos. Struct. 1 (4) (2019) 042001, http://dx.doi.org/10.1088/2631-6331/ab5571.

[5] David Carlstedt, Leif E. Asp, Performance analysis framework for structural battery composites in electric vehicles, Compos. Part B: Eng. 186 (2020) 107822, http://dx.doi.org/10.1016/j.compositesb.2020.107822.

[6] Pias Kumar Biswas, Asel Ananda Habarakada Liyanage, Mayur Jadhav, Mangilal Agarwal, Hamid Dalir, Higher strength carbon fiber lithium-ion polymer battery embedded multifunctional composites for structural applications, Polym. Compos. 43 (5) (2022) 2952–2962, http://dx.doi.org/10.1002/pc.26589.

[7] Koranat Pattarakunnan, Joel Galos, Rajarshi Das, AP Mouritz, Tensile properties of multifunctional composites embedded with lithium-ion polymer batteries, Compos. Part A: Appl. Sci. Manuf. 136 (2020) 105966, http://dx.doi.org/10.1016/j.compositesa.2020.105966.

[8] P. Attar, Joel Galos, A.S. Best, A.P. Mouritz, Compression properties of multifunctional composite structures with embedded lithium-ion polymer batteries, Compos. Struct. 237 (2020) 111937, http://dx.doi.org/10.1016/j.compstruct.2020.111937.

[9] Joel Galos, A.S. Best, A.P. Mouritz, Multifunctional sandwich composites containing embedded lithium-ion polymer batteries under bending loads, Mater. Des. 185 (2020) 108228, http://dx.doi.org/10.1016/j.matdes.2019.108228.

[10] Koranat Pattarakunnan, Joel Galos, Raj Das, A.P. Mouritz, Impact damage tolerance of energy storage composite structures containing lithium-ion polymer batteries, Compos. Struct. 267 (2021) 113845, http://dx.doi.org/10.1016/j.compstruct.2021.113845.

[11] Dian Zhou, Honggang Li, Zhihao Li, Chao Zhang, Toward the performance evolution of lithium-ion battery upon impact loading, Electrochim. Acta 432 (2022) 141192, http://dx.doi.org/10.1016/j.electacta.2022.141192.

[12] Honggang Li, Dian Zhou, Junchao Cao, Zhihao Li, Chao Zhang, On the damage and performance degradation of multifunctional sandwich structure embedded with lithium-ion batteries under impact loading, J. Power Sources 581 (2023) 233509, http://dx.doi.org/10.1016/j.jpowsour.2023.233509.

[13] Joel Galos, Akbar Afaghi Khatibi, Adrian P. Mouritz, Vibration and acoustic properties of composites with embedded lithium-ion polymer batteries, Compos. Struct. 220 (2019) 677–686, http://dx.doi.org/10.1016/j.compstruct.2019.04.013.

[14] Zhongbao Wei, Jiyun Zhao, Hongwen He, Guanglin Ding, Haoyong Cui, Longcheng Liu, Future smart battery and management: Advanced sensing from external to embedded multi-dimensional measurement, J. Power Sources 489 (2021) 229462, http://dx.doi.org/10.1016/j.jpowsour.2021.229462.

[15] Qianqian Meng, Yongxin Huang, Li Li, Feng Wu, Renjie Chen, Smart batteries for powering the future, Joule 8 (2) (2024) 344–373, http://dx.doi.org/10.1016/j.joule.2024.01.011.

[16] Yao Lu, Xiaodan Wang, Shuoyuan Mao, Depeng Wang, Daoming Sun, Yukun Sun, Anyu Su, Chenzi Zhao, Xuebing Han, Kuijie Li, et al., Smart batteries enabled by implanted flexible sensors, Energy Environ. Sci. 16 (6) (2023) 2448–2463, http://dx.doi.org/10.1039/D3EE00695F.

[17] Hossein Montazerian, Armin Rashidi, Abbas S Milani, Mina Hoorfar, Integrated sensors in advanced composites: A critical review, Crit. Rev. Solid State Mater. Sci. 45 (3) (2020) 187–238, http://dx.doi.org/10.1080/10408436.2019.1588705.

[18] R. Janeliukstis, D. Mironovs, Smart composite structures with embedded sensors for load and damage monitoring–a review, Mech. Compos. Mater. 57 (2) (2021) 131–152, http://dx.doi.org/10.1007/s11029-021-09941-6.

[19] Peter W.R. Beaumont, The structural integrity of composite materials and long-life implementation of composite structures, Appl. Compos. Mater. 27 (5) (2020) 449–478, http://dx.doi.org/10.1007/s10443-020-09822-6.

[20] Bo Nie, Jonghan Lim, Tengxiao Liu, Ilya Kovalenko, Kaixuan Guo, Junfei Liang, Jian Zhu, Hongtao Sun, Multifunctional composite designs for structural energy storage, Batter. Energy 2 (6) (2023) 20230023, http://dx.doi.org/10.1002/bte2.20230023.

[21] Alexander Vereen, Austin RJ Downey, Subramani Sockalingam, Simon Laflamme, Validation of large area capacitive sensors for impact damage assessment, Meas. Sci. Technol. 35 (3) (2023) 035106, http://dx.doi.org/10.1088/1361-6501/ad0954.

[22] Leon Prochowski, Mateusz Ziubiński, Krzysztof Dziewiecki, Patryk Szwajkowski, Impact energy and the risk of injury to motorcar occupants in the front-to-side vehicle collision, Nonlinear Dynam. 110 (4) (2022) 3333–3354, http://dx.doi.org/10.1007/s11071-022-07779-8.

[23] Xiuchen Xu, Hongchao Zhang, Xiaobo Du, Qiang Liu, Vehicle collision with RC structures: A state-of-the-art review, in: Structures, vol. 44, Elsevier, 2022, pp. 1617–1635, http://dx.doi.org/10.1016/j.istruc.2022.08.107.

[24] Thomas Kisters, Elham Sahraei, Tomasz Wierzbicki, Dynamic impact tests on lithium-ion cells, Int. J. Impact Eng. 108 (2017) 205–216, http://dx.doi.org/10.1016/j.ijimpeng.2017.04.025.

[25] Shoujun Xi, Qiancheng Zhao, Lijun Chang, Xingyuan Huang, Zhihua Cai, The dynamic failure mechanism of a lithium-ion battery at different impact velocity, Eng. Fail. Anal. 116 (2020) 104747, http://dx.doi.org/10.1016/j.engfailanal.2020.104747.

[26] Bentang Arief Budiman, Samuel Rahardian, Andy Saputro, Arif Hidayat, Ignatius Pulung Nurprasetio, Poetro Sambegoro, Structural integrity of lithium-ion pouch battery subjected to three-point bending, Eng. Fail. Anal. 138 (2022) 106307, http://dx.doi.org/10.1016/j.engfailanal.2022.106307.

[27] Joel Galos, Koranat Pattarakunnan, Adam S Best, Ilias L Kyratzis, Chun-Hui Wang, Adrian P Mouritz, Energy storage structural composites with integrated lithium-ion batteries: a review, Adv. Mater. Technol. 6 (8) (2021) 2001059, http://dx.doi.org/10.1002/admt.202001059.

[28] Jinrui Ye, Xiaolong Ji, Zhendong Liu, Kai Liu, Jun Li, Rengang Wang, Jingkang Wang, Qin Lei, Carbon fiber reinforced structural battery composites: Progress and challenges toward industrial application, Compos. Part B: Eng. (2024) 111411, http://dx.doi.org/10.1016/j.compositesb.2024.111411.

[29] Jin Yan, Austin Downey, An Chen, Simon Laflamme, Sammy Hassan, Capacitance-based sensor with layered carbon-fiber reinforced polymer and titania-filled epoxy, Compos. Struct. 227 (2019) 111247, http://dx.doi.org/10.1016/j.compstruct.2019.111247.

[30] Yanfang Xu, Weibang Lu, Guangbiao Xu, Tsu-Wei Chou, Structural supercapacitor composites: A review, Compos. Sci. Technol. 204 (2021) 108636, http://dx.doi.org/10.1016/j.compscitech.2020.108636.

[31] Hanmo Zhou, Hao Li, Liuqing Li, Tiancheng Liu, Gao Chen, Yanping Zhu, Limin Zhou, Haitao Huang, Structural composite energy storage devices—a review, Mater. Today Energy 24 (2022) 100924, http://dx.doi.org/10.1016/j.mtener.2021.100924.

[32] Kathleen Moyer, Chuanzhe Meng, Breeanne Marshall, Osama Assal, Janna Eaves, Daniel Perez, Ryan Karkkainen, Luke Roberson, Cary L Pint, Carbon fiber reinforced structural lithium-ion battery composite: Multifunctional power integration for CubeSats, Energy Storage Mater. 24 (2020) 676–681, http://dx.doi.org/10.1016/j.ensm.2019.08.003.

[33] Shikha Yadav, Zunjarrao Kamble, Bijoya Kumar Behera, Advances in multifunctional textile structural power composites: a review, J. Mater. Sci. 57 (36) (2022) 17105–17138, http://dx.doi.org/10.1007/s10853-022-07713-8.

[34] Sdiq Anwar Taher, Jian Li, Jong-Hyun Jeong, Simon Laflamme, Hongki Jo, Caroline Bennett, William N Collins, Austin RJ Downey, Structural health monitoring of fatigue cracks for steel bridges with wireless large-area strain sensors, Sensors 22 (14) (2022) 5076, http://dx.doi.org/10.3390/s22145076.

[35] Emmanuel Ogunniyi, Alexander Vareen, Austin RJ Downey, Simon Laflamme, Jian Li, Caroline Bennett, William Collins, Hongki Jo, Alexander Henderson, Paul Ziehl, Investigation of electrically isolated capacitive sensing skins on concrete to reduce structure/sensor capacitive coupling, Meas. Sci. Technol. 34 (5) (2023) 055113, http://dx.doi.org/10.1088/1361-6501/acbb97.

[36] Mohammadkazem Sadoughi, Austin Downey, Jin Yan, Chao Hu, Simon Laflamme, Reconstruction of unidirectional strain maps via iterative signal fusion for mesoscale structures monitored by a sensing skin, Mech. Syst. Signal Process. 112 (2018) 401–416, http://dx.doi.org/10.1016/j.ymssp.2018.04.023.

[37] Xiangxiong Kong, Jian Li, William Collins, Caroline Bennett, Simon Laflamme, Hongki Jo, A large-area strain sensing technology for monitoring fatigue cracks in steel bridges, Smart Mater. Struct. 26 (8) (2017) 085024, http://dx.doi.org/10.1088/1361-665X/aa75ef.

[38] Austin Downey, Anna Laura Pisello, Elena Fortunati, Claudia Fabiani, Francesca Luzi, Luigi Torre, Filippo Ubertini, Simon Laflamme, Durability and weatherability of a styrene-ethylene-butylene-styrene (SEBS) block copolymer-based sensing skin for civil infrastructure applications, Sensors Actuators A: Phys. 293 (2019) 269–280, http://dx.doi.org/10.1016/j.sna.2019.04.022.

[39] Han Liu, Simon Laflamme, Jian Li, Caroline Bennett, William N Collins, Austin Downey, Paul Ziehl, Hongki Jo, Soft elastomeric capacitor for angular rotation sensing in steel components, Sensors 21 (21) (2021) 7017, http://dx.doi.org/10.3390/s21217017.

[40] D7136 D7136/D7136M, Standard test method for measuring the damage resistance of a fiber-reinforced polymer matrix composite to a drop-weight impact event, ASTM Int. (2017).

[41] Xiaoqing Zhu, Hsin Wang, Srikanth Allu, Yanfei Gao, Ercan Cakmak, Emma J Hopkins, Gabriel M Veith, Zhenpo Wang, Investigation on capacity loss mechanisms of lithium-ion pouch cells under mechanical indentation conditions, J. Power Sources 465 (2020) 228314, http://dx.doi.org/10.1016/j.jpowsour.2020.228314.

[42] Hanfeng Yin, Shuai Ma, Honggang Li, Guilin Wen, Shriram Santhanagopalan, Chao Zhang, Modeling strategy for progressive failure prediction in lithium-ion batteries under mechanical abuse, ETransportation 7 (2021) 100098, http://dx.doi.org/10.1016/j.etran.2020.100098.

[43] Honggang Li, Dian Zhou, Chunlin Du, Chao Zhang, Parametric study on the safety behavior of mechanically induced short circuit for lithium-ion pouch batteries, J. Electrochem. Energy Convers. Storage 18 (2) (2021) 020904, http://dx.doi.org/10.1115/1.4048705.

[44] Elze Porte, Sophia Eristoff, Anjali Agrawala, Rebecca Kramer-Bottiglio, Characterization of temperature and humidity dependence in soft elastomer behavior, Soft Robot. 11 (1) (2024) 118–130, http://dx.doi.org/10.1089/soro.2023.0004.

[45] Shuai Ma, Modi Jiang, Peng Tao, Chengyi Song, Jianbo Wu, Jun Wang, Tao Deng, Wen Shang, Temperature effect and thermal impact in lithium-ion batteries: A review, Prog. Nat. Sci.: Mater. Int. 28 (6) (2018) 653–666, http://dx.doi.org/10.1016/j.pnsc.2018.11.002.

[46] Maria Cortada-Torbellino, David Garcia Elvira, Abdelali El Aroudi, Hugo Valderrama-Blavi, Review of lithium-ion battery internal changes due to mechanical loading, Batteries 10 (7) (2024) 258, http://dx.doi.org/10.3390/batteries10070258.

[47] Kyungbae Kim, Candace K. Chan, Design parameters affecting mechanical failure and electrochemical degradation of ultrathin Li-ion pouch cells under repeated flexing, Front. Batter. Electrochem. 3 (2024) 1371167, http://dx.doi.org/10.3389/fbael.2024.1371167.

[48] Sahithi Maddipatla, Lingxi Kong, Michael Pecht, Electrolyte leakage in cylindrical lithium-ion batteries subjected to temperature cycling, Energies 17 (7) (2024) 1533, http://dx.doi.org/10.3390/en17071533.

[49] Elze Porte, Rebecca Kramer-Bottiglio, Nonlinear Poisson's ratio for modeling hyperelastic capacitive sensors, Adv. Mater. Technol. 6 (8) (2021) 2001247, http://dx.doi.org/10.1002/admt.202001247.

[50] Emmanuel A Ogunniyi, Austin RJ Downey Jr., Han Liu, Simon Laflamme, Subramani Sockalingam, Impact monitoring of embedded batteries in sandwich composites with integrated soft elastomeric capacitors, in: Health Monitoring of Structural and Biological Systems XIX, vol. 13437, SPIE, 2025, pp. 346–358, http://dx.doi.org/10.1117/12.3051262.